# Metabolic remodeling in the right ventricle of rats with severe pulmonary arterial hypertension

SEIICHIRO SAKAO[1], EIRYO KAWAKAMI[2], HIROKI SHOJI[1], AKIRA NAITO[1], HIDEKI MIWA[1], RIKA SUDA[1], TAKAYUKI JUJO SANADA[1], NOBUHIRO TANABE[1] and KOICHIRO TATSUMI[1]

[1]Department of Respirology (B2) and [2]Artificial Intelligence Medicine, Graduate School of Medicine, Chiba University, Chiba 260-8670, Japan

Received March 19, 2020; Accepted October 13, 2020

DOI: 10.3892/mmr.2021.11866

**Abstract.** It is generally considered that there is an increase in glycolysis in the hypertrophied right ventricle (RV) during pulmonary hypertension (PH), which leads to a decrease in glucose oxidation through the tricarboxylic acid (TCA) cycle. Although recent studies have demonstrated that fatty acid (FA) and glucose accumulated in the RV of patients with PH, the details of this remain to be elucidated. The purpose of the current study was to assess the metabolic remodeling in the RV of rats with PH using a metabolic analysis. Male rats were treated with the vascular endothelial growth factor receptor blocker SU5416 followed by 3 weeks of hypoxic conditions and 5 weeks of normoxic conditions (Su/Hx rats). Hemodynamic measurements were conducted, and the RV was harvested for the measurement of metabolites. A metabolomics analysis revealed a decreasing trend in the levels of alanine, argininosuccinic acid and downstream TCA cycle intermediates, including fumaric and malic acid and an increasing trend in branched-chain amino acids (BCAAs) in Su/Hx rats compared with the controls; however, no trends in glycolysis were indicated. The FA metabolomics analysis also revealed a decreasing trend in the levels of long-chain acylcarnitines, which transport FA from the cytosol to the mitochondria and are essential for beta-oxidation. The current study demonstrated that the TCA cycle was less activated because of a decreasing trend in the expression of fumaric acid and malic acid, which might be attributable to the expression of adenylosuccinic acid and argininosuccinic acid. These results suggest that dysregulated BCAA metabolism and a decrease in FA oxidation might contribute to the reduction of the TCA cycle reactions.

*Correspondence to:* Professor Seiichiro Sakao, Department of Respirology (B2), Graduate School of Medicine, Chiba University, 1-8-1 Inohana, Chuo-ku, Chiba 260-8670, Japan
E-mail: sakaos@faculty.chiba-u.jp

*Abbreviations:* BCAAs, branched-chain amino acids; BMIPP, $^{123}$I-β-methyl iodophenyl pentadecanoic acid; CTEPH, chronic thrombombolic pulmonary hypertension; FA, fatty acid; HCA, Hierarchical cluster analysis; PA, pulmonary arterial; PAH, pulmonary arterial hypertension; PCA, principal component analysis; PH, pulmonary hypertension; RV, right ventricle; RVSP, RV systolic pressure; TCA cycle, the tricarboxylic acid cycle

*Key words:* metabolic remodeling, right ventricle, pulmonary hypertension, SU5416

## Introduction

Various factors, such as the genetic background and biological environment, are suggested to induce vasoconstriction of the pulmonary arteries and cell proliferation in pulmonary vasculature in many forms of pulmonary hypertension (PH) (1-3). This leads to stenosis and obstruction of the vascular lumen, resulting in an increase in the pulmonary arterial (PA) pressure (4). In accordance with the increase in pressure, the right heart function decreases, leading to right heart failure, which eventually becomes a prognostic factor in these patients (5,6).

Metabolic remodeling has been described not only in pulmonary artery vascular cells but also in the right ventricle cardiomyocytes of pulmonary arterial hypertension (PAH) (7). The metabolic alterations include mitochondrial inactivation, which leads to the suppression of glucose oxidation through the tricarboxylic acid (TCA) cycle and upregulation of normoxic glycolysis (8,9).

Fatty acid (FA) oxidation is suggested to be the major source of energy production, especially in the left ventricle. Indeed, it is responsible for 60-90% of ATP synthesis (10). Although the details of FA metabolism in the hypertrophied RV in PH remain unclear, our recent studies using positron emission tomography (PET) and $^{123}$I-β-methyl iodophenyl pentadecanoic acid (BMIPP) uptake imaging have revealed the accumulation of not only glucose but also FA in the RV of patients with chronic thromboembolic pulmonary hypertension (CTEPH) (11,12). However, these studies only showed the accumulation of FA in the cytoplasm, and whether or not FA oxidation actually occurs through the TCA cycle in mitochondria has remained unclear.

FA oxidation in the hypertrophied RV in PH is still controversial. An increase in FA oxidation in the RV was shown in the PA banding model (13). However, a reduction in FA oxidation was noted in both the adaptive and maladaptive RV in the monocrotaline rat model and the PA banding model (14-16). In addition, impaired FA transport into the

stressed myocardium has been demonstrated in a PAH model with right heart failure, which was developed by treatment with a vascular endothelial growth factor receptor blocker (SUGEN5416), followed by exposure to chronic hypoxia (Su/Hx) (17).

Metabolomics can comprehensively analyze metabolites induced *in vivo* by the action of proteins. This analysis can reveal the activity of the protein, allowing for the direct monitoring of life phenomena (18). In the present study, we investigated the metabolic remodeling of glucose and FA in the RV of a rat model of PAH (Su/Hx model) via a metabolome analysis.

## Materials and methods

*Animals*. Five-week-old male wild-type Sprague-Dawley rats weighing 100-150 g were purchased from CLEA Japan. All animal studies were approved by the Review Board for Animal Experiments of Chiba University (no. 30-126) and were therefore performed in accordance with the ethical standards laid down in the principles of the NIH Guide for the Care and Use of Laboratory Animals (NIH Publication, 8th edition, 2011).

*Rat model of severe PAH (Su/Hx model)*. PH was induced in rats with a single 20 mg/kg subcutaneous injection of a vascular endothelial growth factor receptor antagonist (SU5416; R&D Systems), followed by 3 weeks of exposure to hypoxic conditions (10% $O_2$) and then 5 weeks of exposure to normoxic conditions, as previously reported (19). Hemodynamic measurements were performed, and the RV was harvested for the measurement of metabolites. All rats were housed in standard cages and had free access to food and water

*Hemodynamic measurements*. Rats were intraperitoneally anesthetized with pentobarbital sodium (30 mg/kg). A polyethylene tube catheter [outer diameter (OD): 1.0 mm; Hibiki] was inserted into the RV through the right jugular vein to measure the RV systolic pressure (RVSP). Signals were monitored with a physiological transducer (NEC Sanei), an amplifier system (NEC Sanei), and recorder (Nihon Kohden). After the hemodynamic measurements, the rats were euthanized with pentobarbital sodium (150 mg/kg). The heart was harvested for the measurement of metabolites, and then the weights of the RV and left ventricle + septum (LV+S) were measured to determine the RV/LV+S ratio.

*Metabolite extraction*

*C-SCOPE*. Metabolite extraction was conducted at Human Metabolome Technologies (HMT). Approximately 32 mg of the frozen RV tissue was plunged into 750 $\mu$l of 50% acetonitrile/Milli-Q water containing internal standards (H3304-1002; HMT) at 0˚C in order to inactivate enzymes. The tissue was homogenized three times at 3,500 rpm for 1 min using a tissue homogenizer (Micro Smash MS100R; Tomy Digital Biology Co., Ltd.) and then the homogenate was centrifuged at 2,300 x g and 4˚C for 5 min. Subsequently, 400 $\mu$l of upper aqueous layer was centrifugally filtered through a Millipore 5-kDa cutoff filter at 9,100 x g and 4˚C for 120 min to remove proteins. The filtrate was centrifugally concentrated and re-suspended in 50 $\mu$l of Milli-Q water for a CE-MS analysis.

*LC-MS*. Metabolite extraction and the metabolome analysis were conducted at HMT. Briefly, approximately 35 mg of the frozen RV tissue was plunged into 500 $\mu$l of 1% formic acid/acetonitrile containing internal standard solution (H3304-1002; HMT) at 0˚C. The tissue was homogenized three times at 1,500 rpm for 120 sec using a tissue homogenizer (Micro Smash MS100R; Tomy Digital Biology Co., Ltd.) and then the homogenate was centrifuged at 2,300 x g and 4˚C for 5 min and the mixture was homogenized again after adding 167 $\mu$l of Milli-Q water. Then the homogenate was centrifuged at 2,300 x g and 4˚C for 5 min. The supernatant was then mixed with 500 $\mu$l of 1% formic acid/acetonitrile and 167 $\mu$l of Milli-Q water, and the solution was filtrated through a 3-kDa cutoff filter (NANOCEP 3K OMEGA; PALL Corporation) to remove macromolecules and further filtrated using a hybrid SPE phospholipid cartridge (55261-U; Supelco) to remove phospholipids. The filtrate was desiccated and then re-suspended in 100 $\mu$l of isopropanol/Milli-Q water for the LC-TOFMS analysis.

*Metabolome analyses*

*C-SCOPE*. The metabolome analyses were conducted with the C-SCOPE package of HMT using capillary electrophoresis time-of-flight mass spectrometry (CE-TOFMS) for the cation analysis and CE-tandem mass spectrometry (CE-MS/MS) for the anion analysis, based on previously described methods (20-23). Briefly, the CE-TOFMS analysis was carried out using an Agilent CE capillary electrophoresis system equipped with an Agilent 6210 time-of-flight mass spectrometer (Agilent Technologies). The systems were controlled by the Agilent G2201AA ChemStation software program (version B.03.01 for CE; Agilent Technologies) and connected by a fused silica capillary (50 $\mu$m i.d. x80 cm total length) with a commercial electrophoresis buffer (H3301-1001 and I3302-1023 for the cation and anion analyses, respectively, HMT) as the electrolyte. The spectrometer scanned from m/z 50 to 1,000 (20). Peaks were extracted using MasterHands, an automatic integration software program (Keio University) (21) and MassHunter Quantitative Analysis B.04.00 (Agilent Technologies) in order to obtain peak information, including m/z, peak area, and migration time (MT). Signal peaks were annotated according to the HMT metabolite database, based on their m/z values with the MTs. The concentrations of metabolites were calculated by normalizing the peak area of each metabolite with respect to the area of the internal standard and using standard curves with three-point calibrations. A hierarchical cluster analysis (HCA) and principal component analysis (PCA) were performed using HMT's proprietary software programs, PeakStat and SampleStat, respectively. The detected metabolites were plotted on metabolic pathway maps using the VANTED software program (23).

*LC-MS*. The metabolome analyses were conducted using the LC-MS package of HMT, based on previously described methods (21-23). Briefly, an LC-TOFMS analysis was carried out using an Agilent LC System (Agilent 1200 series RRLC system SL) equipped with an Agilent

Table I. Evaluation of RV overload in Su/Hx and control rats.

| Rat group | Control-1 | Control-2 | Control-3 | Su/Hx-1 | Su/Hx-2 | Su/Hx-3 | Control | Su/Hx | P-value |
|---|---|---|---|---|---|---|---|---|---|
| BW | 440 | 600 | 565 | 374 | 505 | 442 | 535±84 | 440±66 | 0.199 |
| RVSP | 26.7 | 20 | 18.8 | 61.8 | 53.9 | 50.3 | 21.8±4.3 | 55.3±5.9 | 0.001 |
| RV/LV+S | 0.2 | 0.21 | 0.17 | 0.725 | 0.42 | 0.43 | 0.19±0.02 | 0.53±0.17 | 0.030 |

RV, right ventricle; RVSP, right ventricle systolic pressure; LV+S, left ventricle and septum; BW, body weight.

6230 TOFMS (Agilent Technologies). The systems were controlled by the Agilent G2201AA ChemStation software program (version B.03.01; Agilent Technologies) equipped with an ODS column (2x50 mm, 2 $\mu$m) (21). Peaks were extracted using MasterHands, an automatic integration software program (Keio University) in order to obtain peak information, including m/z, peak area, and retention time (RT) (22). Signal peaks corresponding to isotopomers, adduct ions, and other product ions of known metabolites were excluded, and the remaining peaks were annotated according to the HMT metabolite database, based on their m/z values with the RTs determined by TOFMS. The areas of the annotated peaks were then normalized based on internal standard levels and sample amounts, in order to obtain the relative levels of each metabolite. The HCA and PCA were performed using HMT's proprietary software programs, PeakStat and SampleStat, respectively. Detected metabolites were plotted on metabolic pathway maps using the VANTED software program (23).

*Statistical analyses*. The RV afterload was compared between the groups using Student's t-test. In the metabolome analysis, the mean metabolite concentrations were compared between the groups by the Brunner-Munzel test (24). P values of <0.05 were considered to indicate statistical significance. The SampleStat software program (ver. 3.14; HMT) was used to perform the metabolome analysis. This program does not support scatter/dot plots. Thus, a box-and-whisker plot was used to present these results. For the other statistical analyses, the JMP® (SAS Institute, Inc.) and R software programs (https://cran.r-project.org/src/base/R-4/R-4.0.3.tar.gz) were used. For the hierarchical clustering analysis, the Pearson correlation coefficient was used to evaluate the similarity between metabolite profiles. Ward's method was employed for hierarchical clustering.

## Results

*The evaluation of the RV overload in Su/Hx and control rats*. To evaluate the RV afterload, all animals were subjected to hemodynamic measurements and dissected at the end of the experimental period. The RV hemodynamics were measured by closed chased cannulation of the jugular vein. The RVSP and RV/LV+S in Su/Hx and untreated control rats are presented in Table I. The RVSP in Su/Hx rats was significantly higher than that in untreated controls (55.3±5.9 vs. 21.8±4.3 mmHg, P=0.001), as was the RV/LV+S (0.53±0.17 vs. 0.19±0.02, P=0.030) (Table I).

*The cation and anion analyses by CE-TOFMS and CE-MS/MS*. Metabolome analyses were conducted using CE-TOFMS for the cation analysis and CE-MS/MS for the anion analysis based on previously described methods (20-23). Fig. 1A shows that the principal component analysis (PCA) completely separated the metabolic profiles of Su/Hx and control rats in CE-TOFMS and CE-MS/MS. The principal component (PC) 1 in Fig. 1A was interpreted as treatment condition separation (Su/Hx vs. control rats). Among 84 features obtained by CE-TOFMS and CE-MS/MS, 16 compounds significantly differed between Su/Hx and control rats (Fig. 1B; Brunner-Munzel test: P<0.05). Branched-chain amino acids (BCAAs), including isoleucine, leucine and valine were increased in Su/Hx rats, while the levels of these metabolites, including citric acid, malic acid, fumaric acid, adenylosuccinic acid and argininosuccinic acid showed, a decreasing trend in Su/Hx rats. The level of alanine, a TCA cycle-related amino acid, was lower in the Su/Hx rats than in the control rats.

We identified six major clusters of metabolites using a hierarchical clustering analysis (HCA) based on the Pearson correlation coefficient (Fig. 1C). Since malic acid, fumaric acid, adenylosuccinic acid, argininosuccinic acid and alanine were included in the same cluster (Cluster 5 in Fig. 1C), together with CoA, NADPH, and NADP+, cofactors in anabolic reactions, the metabolic pathway related to these metabolites seemed to be downregulated in Su/Hx rats. On the other hand, BCAAs were in another cluster (Cluster 3 in Fig. 1C), which showed a strong negative correlation with Cluster 1, indicating that BCAAs might be regulated in a coordinated manner in Su/Hx rats.

*A metabolic map of glycolysis and the TCA cycle in the metabolic pathway of Su/Hx and control rats*. To understand the relationships among metabolites that are differentially expressed in Su/Hx rats, we then mapped the metabolites to metabolic pathway maps. The glycolysis pathway map showed no statistically significant differences in any of the intermediates (Fig. 2A and B). These results suggested that the glycolytic metabolic pathway did not differ between the groups.

The TCA cycle map further showed a decreasing trend in the levels of alanine, argininosuccinic acid and intermediates, as well as fumaric acid, malic acid, and citric acid, in the TCA cycle in Su/Hx rats in comparison to control rats (Fig. 2A and B). These results indicated that the TCA cycle in the RV of Su/Hx rats is less active than that in controls.

As noted in the previous section, all BCAAs were increased in Su/Hx rats in comparison to controls (Fig. 2A and B). BCAAs are amino acids with aliphatic side chains with branching

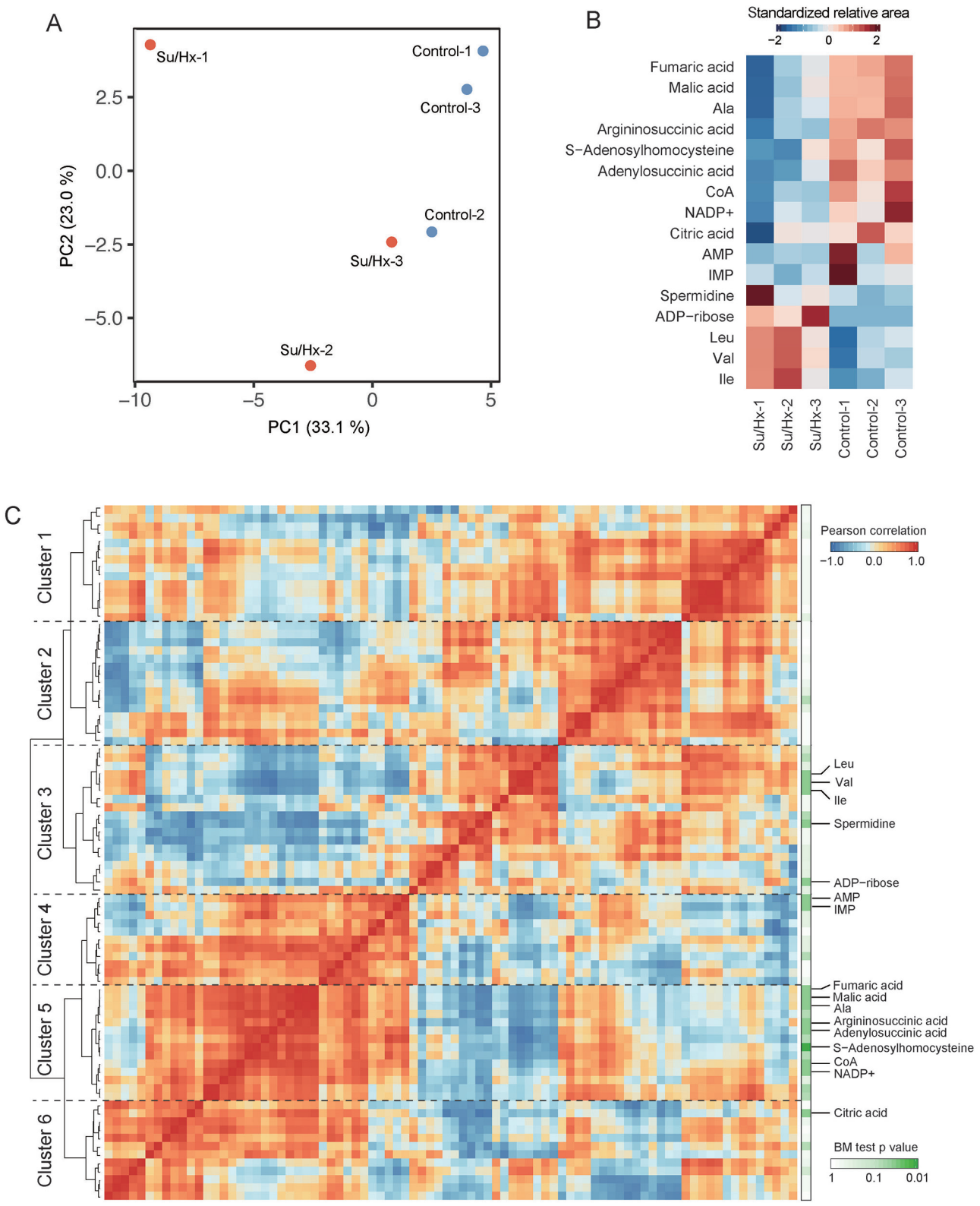


Figure 1. The metabolic profiles of Su/Hx model using CE-TOFMS and CE-MS/MS. (A) Principal component analysis of metabolites measurement using CE-TOFMS and CE-MS/MS from heart of Su/Hx and control rats (n=3 in each group). (B) Heat map illustrating relative expression of metabolites measured with CE-TOFMS and CE-MS/MS that significantly differ between Su/Hx and control rats (Brunner-Munzel test). (C) Hierarchically clustered similarity heat map between 86 metabolites measured with CE-TOFMS and CE-MS/MS. Pearson's correlation coefficient was used to evaluate the similarity between the metabolite expression profiles. P values calculated in Brunner-Munzel test comparing Su/Hx and control rats were indicated using green-white coloring next to the correlation heat map. CE, capillary electrophoresis; TOM, time-of-flight; MS, mass spectrometry.

(binding of two or more other carbon atoms to any carbon atom). Proteinogenic amino acids include three types of BCAA: Leucine, isoleucine, and valine. These three types of BCAAs are essential amino acids in humans. The branched chain α-keto acid dehydrogenase complex (BCKDH) is involved in the cleavage of BCAAs, whereby the BCAA is converted to an

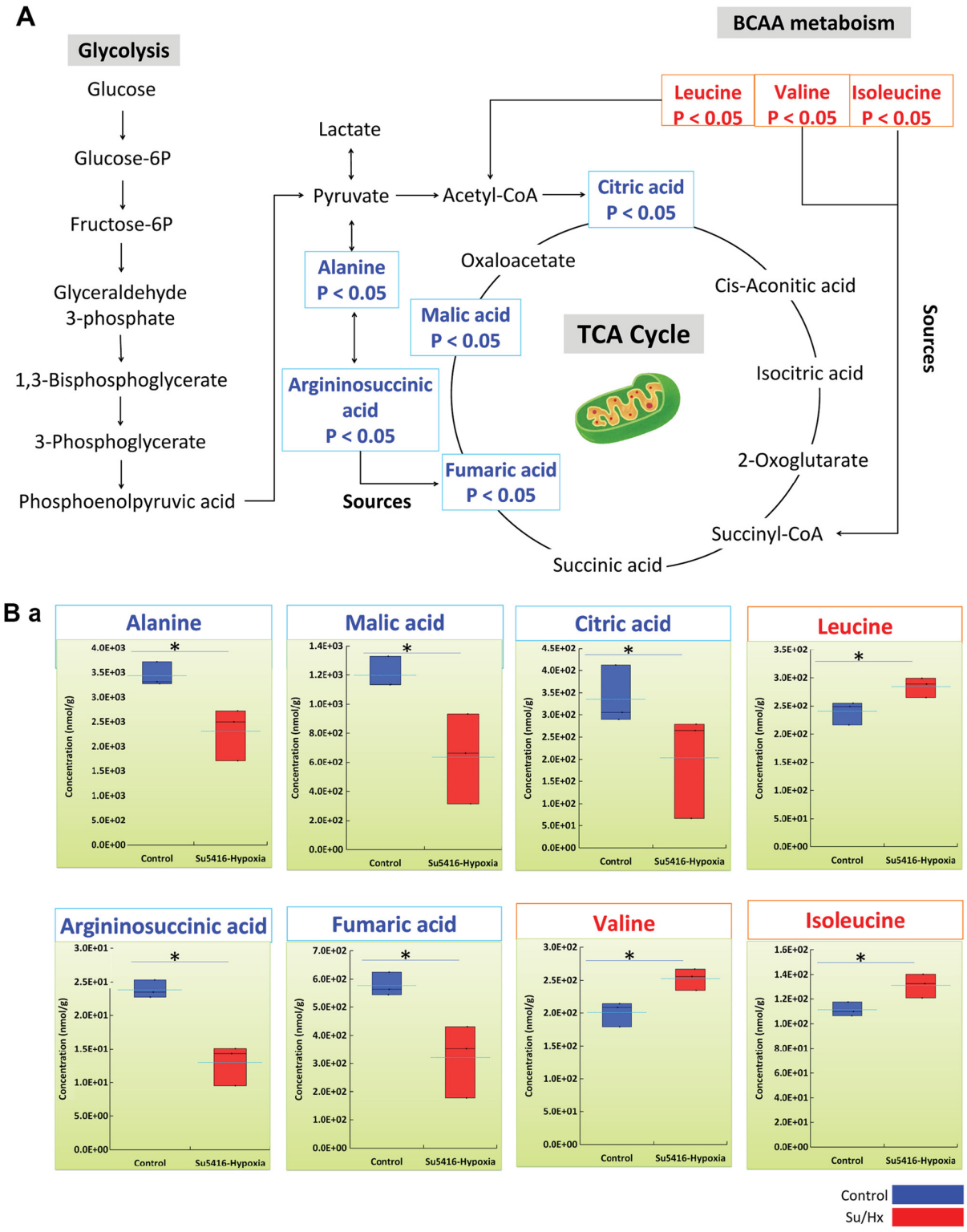


Figure 2. Continued.

acyl CoA derivative, which is subsequently converted to acetyl CoA or succinyl CoA before finally being incorporated into the TCA cycle (Fig. 2A and B). Total BCAA is calculated as the total amount of leucine, isoleucine, and valine, and was found to be significantly increased in Su/Hx rats in comparison to controls (Su/Hx vs. Control; P<0.05) (Fig. 2B).

Several metabolic parameters were calculated based on metabolite measurements in CE-TOFMS and CE-MS/MS to assess the metabolic balance in each pathway. Among them, we observed a number of notable trends.

The NADH to NAD+ Ratio (NADH/NAD+): NAD+ is used as a cofactor necessary for the catalytic activity of the enzyme in many reactions, including glycolysis, citric acid cycle, and β-oxidation of fatty acids. Then, NADH produced as a reactant plays a role in the electron transfer system in ATP production via oxidative phosphorylation. The

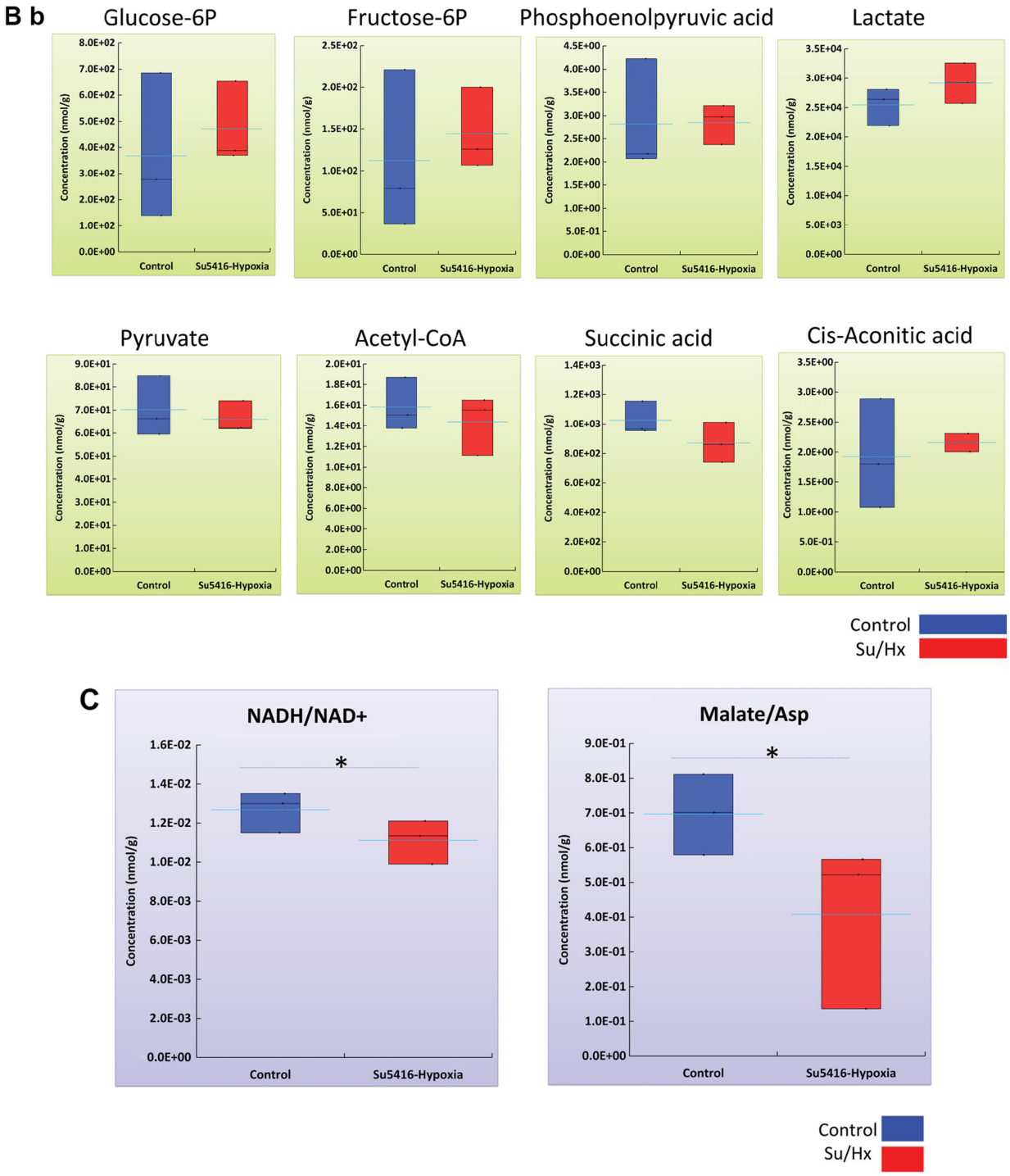


Figure 2. Glycolysis and the TCA cycle in the metabolic pathway. (A) Glycolysis and the TCA cycle in heart of Su/Hx and control rats are shown in the metabolic pathway map (n=3 in each group). (Ba and Bb) Metabolites in the Control and su5416-Hypoxia group (n=3 in each group). (C) Metabolic parameters including NADH to NAD+ ratio (NADH/NAD+), malate to asparate ratio (Malate/Asp), glutathione redox ratio (GSH/GSSG) and lactate to pyruvate ratio (lactate/pyruvate ratio) are presented (n=3 in each group). *P<0.05. TCA, tricarboxylic acid cycle.

NADH/NAD+ ratio is known to decrease during stagnation of central carbon metabolism under hypoxia. The ratio showed a significant decrease in Su/Hx rats in comparison to controls (Su/Hx vs. Control; P<0.05) (Fig. 2C).

The Malate to Aspartic acid Ratio (Malate/Asp): Malic acid is produced from oxaloacetate with a reaction from NADH to NAD+ in the cytoplasm. Conversely, in the mitochondria, it is converted to oxaloacetate in the reaction from NAD+ to NADH. Oxaloacetate is converted to Asp, which is capable of passing from the inner mitochondrial membrane to the cytoplasm, and in the cytoplasm, Asp is converted to oxaloacetate. This cycle is called as the malate-aspartate shuttle, and is a mechanism for transporting NADH, which is required for ATP production by oxidative phosphorylation, from the cytoplasm to the inner mitochondrial membrane. Thus, the Malic acid/Asp ratio is an indirect indicator of

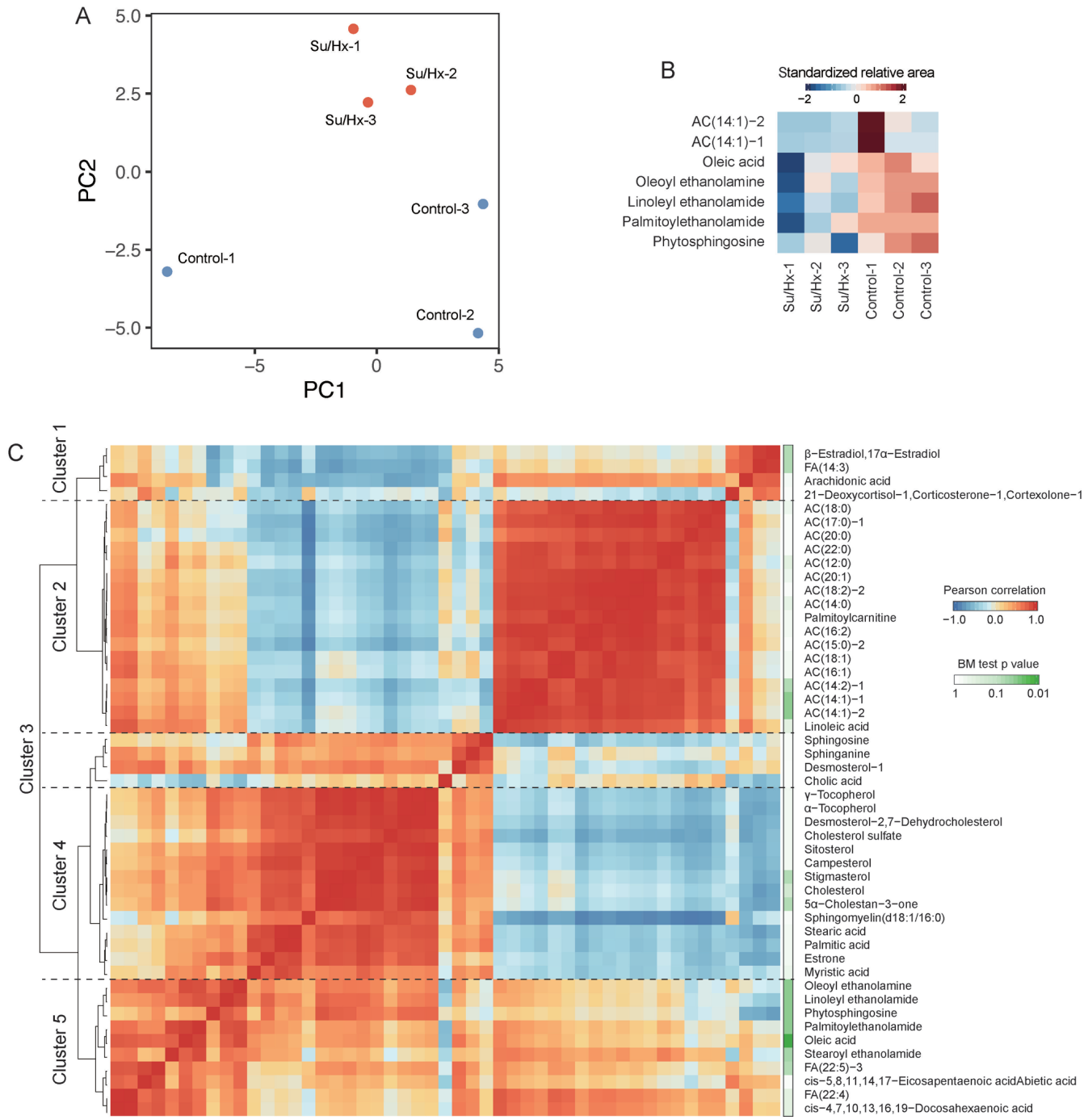


Figure 3. The metabolic profiles of Su/Hx model using LC-TOFMS. (A) Principal component analysis of metabolites measurement using LC-TOFMS from heart of Su/Hx and control rats (n=3 in each group). (B) Heat map illustrating relative expression of metabolites measured with LC-TOFMS that significantly differ between Su/Hx and control rats (Brunner-Munzel test). (C) Hierarchically clustered similarity heat map between 49 metabolites measured with LC-TOFMS. Pearson's correlation coefficient was used to evaluate the similarity between the metabolite expression profiles. P values calculated in Brunner-Munzel test comparing Su/Hx and control rats were indicated using green-white coloring next to the correlation heat map. LC-TOFMS, Liquid chromatography time-of-flight mass spectrometry.

the NADH/NAD + ratio and energy status. There was a significant decrease in Su/Hx rats in comparison to controls (Su/Hx vs. Control; P<0.05) (Fig. 2C).

*The HCA in LC-TOFMS.* Metabolome analyses were conducted using LC-TOFMS for long-chain FAs and long-chain acylcarnitines. FA is known to be an important substrates for energy production and acylcarnitines, as a transporter of FA from the cytosol to mitochondria and to be essential for the entry of FA into β-oxidation (25). The PCA completely separated the metabolic profiles of long-chain FAs and long-chain acylcarnitines of Su/Hx and control rats (Fig. 3A). Among 49 features obtained with LC-TOFMS, 7 compounds showed significant differences between Su/Hx and control rats (Fig. 3B; Brunner-Munzel test: P<0.05). The levels of oleoyl ethanolamine, linoleyl ethanolamide, palmitoylethanolamide and phytosphingosine, in addition to two acylcarnitines, AC(14:1)-1 and AC(14:1)-2, were significantly lower in Su/Hx

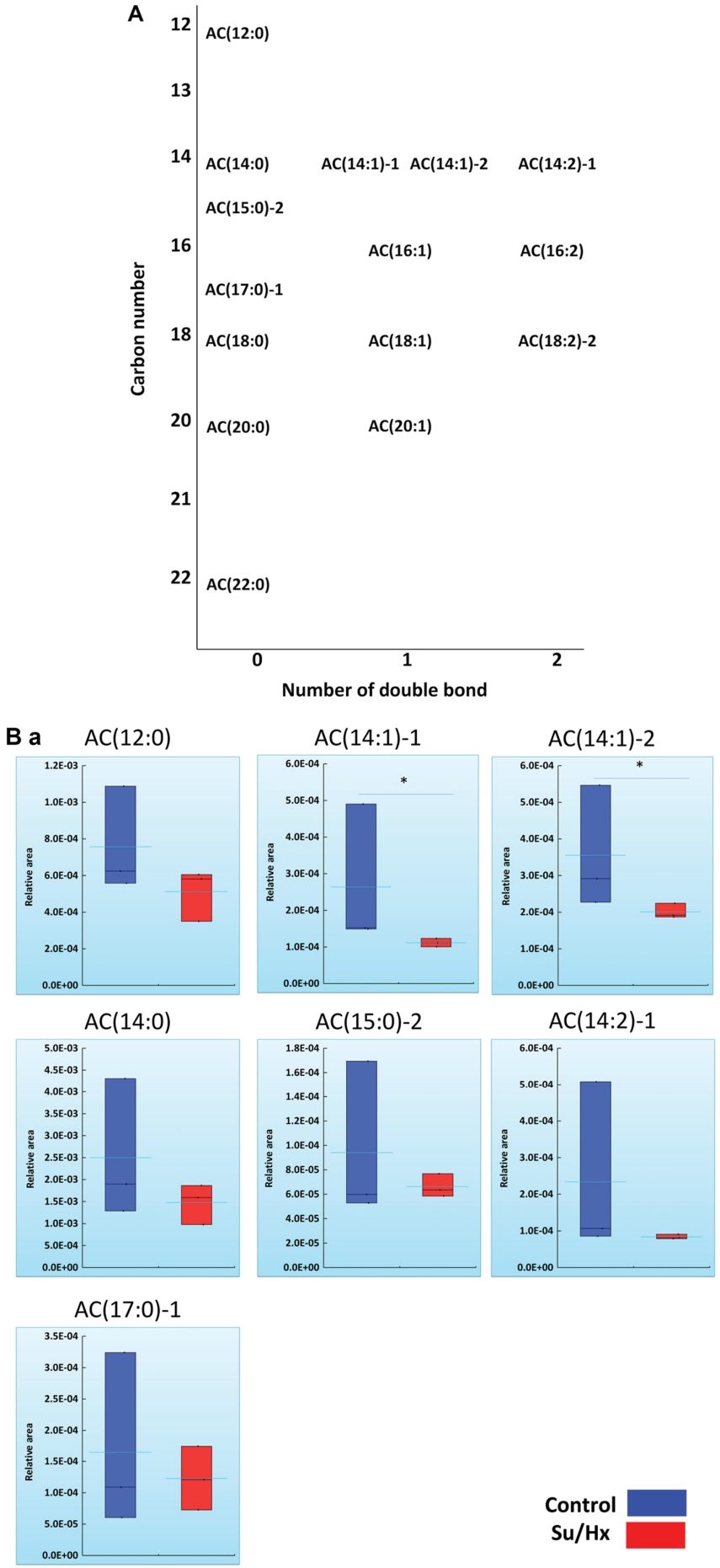


Figure 4. Continued.

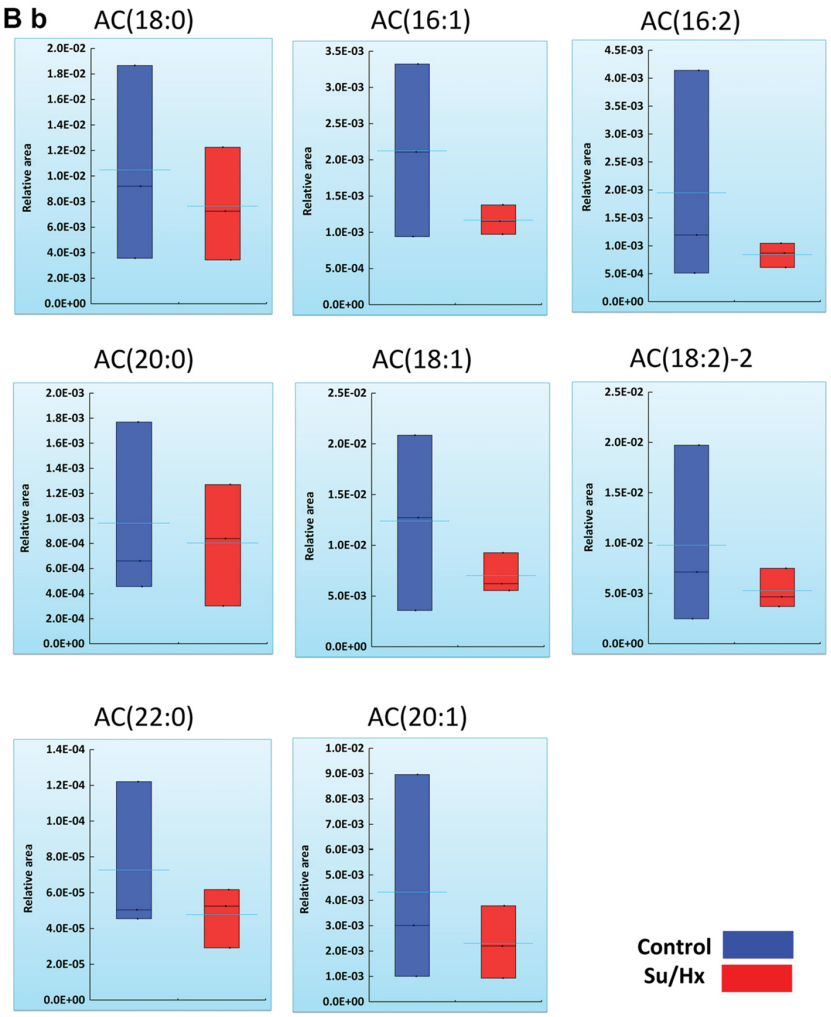


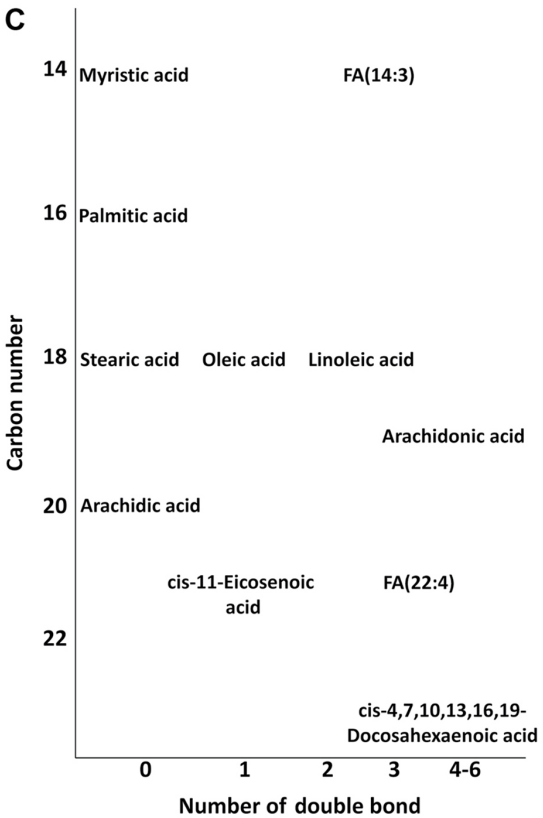


Figure 4. Continued.

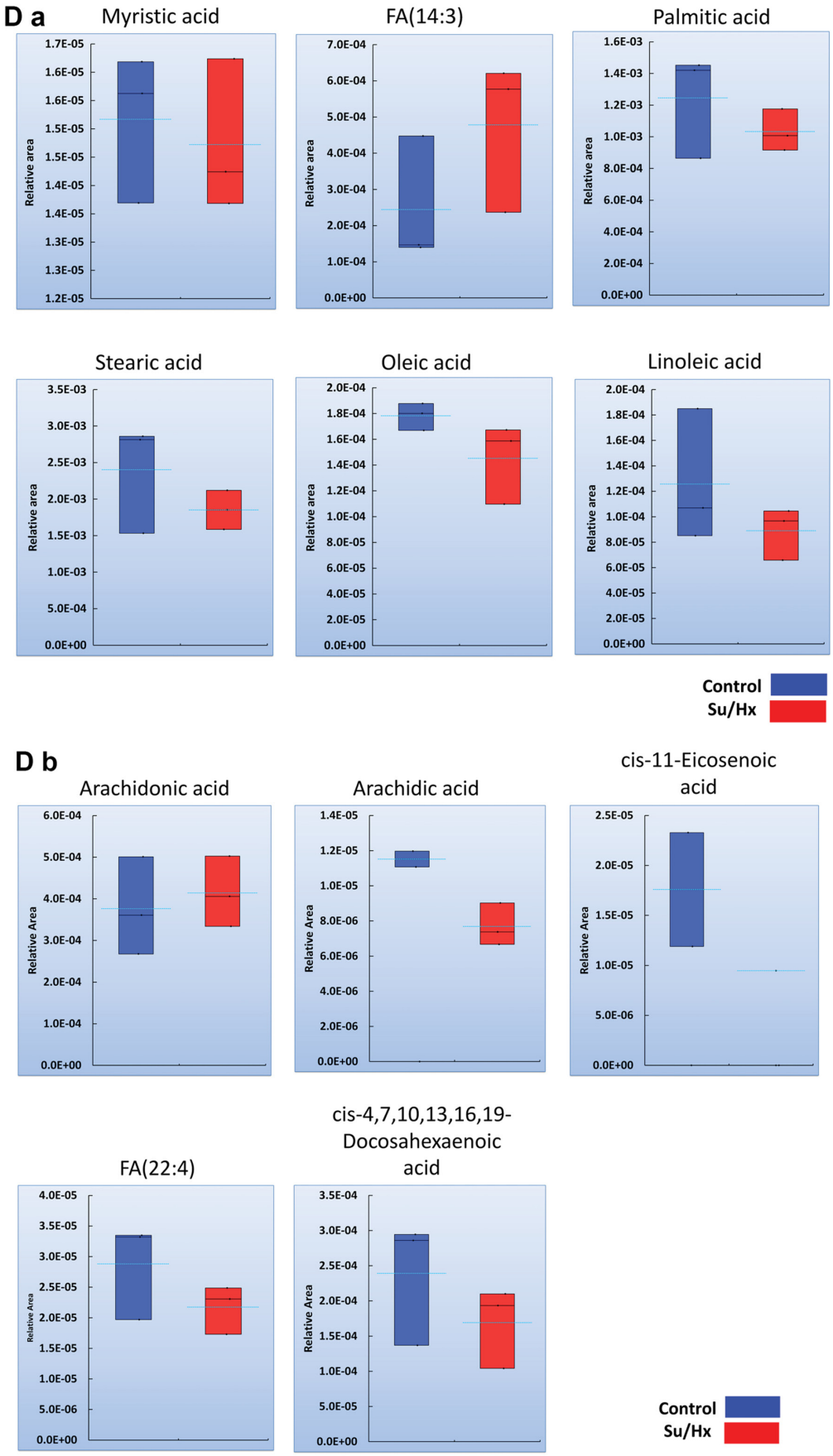


Figure 4. Long-chain ACs and FA profiles in Su/Hx and control rats. (A) An LC-TOFMS analysis for the RV in the groups revealed statistical differences in AC(14:1)-1 and AC(14:1)-2 in Su/Hx rats compared with control rats and a decreasing trend in the levels of other long-chain acylcarnitines (n=3 in each group). (Ba and Bb) The bar graphs of Long-chain acylcarnitines (n=3 in each group). (C) No marked differences in the cytoplasm concentration of long-chain FAs were noted between Su/Hx and control rats. (Da and Db) The bar graphs of long-chain FAs (n=3 in each group). $^{*}P<0.05$; AC, acylcarnitines; FA, fatty acids; LC-TOFMS, Liquid chromatography time-of-flight mass spectrometry.

rats than in control rats. The long-chain FAs and long-chain acylcarnitines were grouped into five clusters by the HCA, based on the Pearson correlation coefficient (Fig. 3C). The biggest cluster, Cluster 2, contains all of long-chain acylcarnitines indicating the common regulation. Since Oleoyl ethanolamine, linoleyl ethanolamide, palmitoylethanolamide and phytosphingosine were located adjacent to each other in Cluster 5, it was suggested that these metabolites were involved in similar pathways.

*Long-chain acylcarnitines and FA profiles in Su/Hx and control rats*. Among 15 long-chain acylcarnitines, FA metabolomics revealed statistically significant differences in AC(14:1)-1 and AC(14:1)-2 in Su/Hx rats in comparison to control rats and a decreasing trend in the levels of other long-chain acylcarnitines (Fig. 4A and B). Long-chain FAs are hydrolyzed to acyl-CoAs by mitochondrial acyl-CoA synthase, after which carnitine palmitoyltransferase 1 (CPT1) converts the acyl-CoAs to long-chain acylcarnitines (26). No marked differences in the cytoplasm concentrations of long-chain FAs were noted between Su/Hx and control rats (Fig. 4C and D). Despite this lack of a marked difference in FAs, the decrease in the levels of long-chain acylcarnitines in the RV of Su/Hx rats might reflect dysregulated β-oxidation.

## Discussion

The current study showed that although there was almost no difference in the glycolytic metabolic pathway (Fig. 2A and B), the TCA cycle in the RV of Su/Hx rats was less active in comparison to controls (Fig. 2A and B). In addition, the levels of long-chain acylcarnitines in the RV of Su/Hx rats tended to be lower than those in controls (Fig. 4A and B). These results suggested that the glycolytic and fatty acid metabolic pathway might be dysregulated and supported that the disordered RV in Su/Hx rats was the result of multilevel failure of FA metabolism (17). However, no marked differences in the concentration of long-chain FAs were noted between the Su/Hx and control rats.

It is true that the TCA cycle was less active because of a decreasing trend in the levels of fumaric acid, malic acid and citric acid. However, it is also important that cis-aconitic acid and succinic acid showed almost no difference between the groups. As shown in Figs. 1B and 2, the current analysis demonstrated that there was a decrease in the level of adenylosuccinic acid and argininosuccinic acid, which were involved in the metabolic pathway of alanine, aspartate and glutamate, and which are transformed into fumaric acid (27). It is hypothesized that the decrease in the level of fumaric acid might be attributable to the expression levels of adenylosuccinic acid and argininosuccinic acid.

Our recent studies using $^{123}$I-BMIPP uptake imaging revealed the FA accumulation in the RV of patients with CTEPH, although whether or not the accumulated FAs actually function as a substrate for ATP synthesis through the TCA cycle in mitochondria remained unclear (11,12). One possible explanation for these discrepant results between the present and previous studies may be differences in the adaptability of the RV to an increased afterload. In patients with CTEPH, successful thromboendarterectomy is able to reverse the RV function and reduce the increased FA accumulation in the RV, suggesting that there is some degree of adaptive capacity in response to the altered FA metabolism in the RV of patients with CTEPH. In contrast, in patients with a severely impaired RV with a low ejection fraction, the RV might be maladaptive to a severely increased afterload. Indeed, the decreased accumulation of FA has been demonstrated in the severely hypertrophied RV with a reduced systolic function in patients with PH, suggesting that a maladaptive RV may possess metabolic alterations, including decreased FA β-oxidation (28).

Bogaard *et al* (29) showed that, in the RV myocardium of the Su/Hx rat model, fatal RV failure, including myocardial apoptosis, fibrosis and a decreased RV capillary density, developed, whereas no such failure was noted in a rat model with PA banding that induced only chronic progressive RV pressure overload. The Su/Hx rat model, which is an established model of angioproliferative PH, is suggested to induce RV alterations, in addition to changes due to isolated RV pressure overload alone, which may include FA metabolic remodeling. These are several possible reasons for the difference in the FA kinetics in the RV between our Su/Hx model and actual patients with CTEPH.

The present study showed that there were decreases in the levels of downstream TCA cycle intermediates, including fumaric acid and malic acid. These metabolites were categorized into the same cluster in the HCA analysis based on CE-TOFMS and CE-MS/MS data (Fig. 1C). The quantitative metabolome analysis revealed decreased levels of fumaric acid (Su/Hx vs. Control; $P<0.05$) and malic acid (Su/Hx vs. Control; $P<0.05$) and increased levels of leucine (Su/Hx vs. Control; $P<0.05$), valine (Su/Hx vs. Control; $P<0.05$) and isoleucine (Su/Hx vs. Control; $P<0.05$) (absolute values; Fig. 2A and B). Although valine and isoleucine, which were subsequently converted to succinyl CoA, increased in Su/Hx rats, decreasing trends were noted in the levels of downstream TCA cycle intermediates after succinyl CoA (Fig. 2A and B). Our findings suggested that the flow from BCAAs to the TCA cycle may be suppressed.

The quantitative metabolome analysis showed that the levels of metabolites such as adenylosuccinic acid and argininosuccinic acid were significantly lower in Su/Hx rats than in controls (Su/Hx vs. Control; $P<0.050$, $P<0.05$). Recently, it was shown that argininosuccinic acid is synthesized directly from fumaric acid (30). The reduction in the level of arginosuccinic acid may be associated with a decrease in the level of fumaric acid, an intermediate in the TCA cycle. Arginosuccinic acid is a metabolic intermediate of the urea cycle, and the results of the present study suggested that the TCA cycle and the urea cycle may be suppressed in the RV of Su/Hx rats. However, whether or not adenylosuccinic acid is involved in the progression of RV remodeling remains unclear.

In the PCA based on LC-TOFMS data, Control-1 was plotted in separate locations despite being prepared in the same experiment (Fig. 3A). We must therefore consider the possibility that some outliers were included in the sample. In normal controls, metabolites targeted in the LC-TOFMS analysis may be easily altered in certain environmental conditions. In Su/Hx rats, however, it should be meaningful that each one had almost the same metabolic background (Fig. 3A).

Several recent studies have explored the utility of plasma metabolites as biomarkers for PH (31,32). Lewis *et al* showed

that some plasma metabolites were useful as biomarkers reflecting RV and pulmonary vascular dysfunction in patients with PAH (31). Rhodes *et al* (32) demonstrated a relationship between the metabolic profile and the outcomes of patients with PAH. Both studies also detected increased levels of TCA cycle intermediates, suggesting that glucose oxidation was upregulated in patients with PAH. In the present study, however, conflicting results were confirmed in the RV of Su/Hx PAH rats. It is suspected that plasma metabolites can, to some extent, reflect the pathophysiological features of organ-specific disease. However, plasma metabolites also reflect metabolites from all types of cells exposed to the PH-induced microenvironment. Although the metabolites detected in the current study cannot be used as PH biomarkers, they may directly reflect the metabolism of the dysfunctional RV in PAH.

It is generally acknowledged that, in the condition with hypoxia, there is an increase in glycolysis, leading to a decrease in glucose oxidation through the tricarboxylic acid (TCA) cycle. Only the hypoxic condition can induce the increase of pulmonary arterial pressure in rat models. Therefore, the metabolic remodeling as an increase in glycolysis is supposed to occur in RV. However, it remains uncertain whether the metabolic remodeling in RV are changed according to the condition with normoxia or hypoxia.

The current study, there are some limitations. First, the total number of rats was extremely small. Because metabolome analyses including C-SCOPE and LC-MS cost a fortune, but our budget was limited. Second, there was the lack of mitochondrial staining experiments. We tried to confirm differences of mitochondrial form between control and Su/Hx rats RV cardiomyocytes by using MitoTracker Red, which is a red-fluorescent dye that stains mitochondria. However, it was impossible to confirm mitochondrial formation by using RV tissue. To detect mitochondria clearly, cultured single layered cells from RV should be needed. However, it was impossible to isolate live RV cardiomyocytes from the tissues. Third, in the current study, we analyzed only the RV, not LV. Because right heart failure eventually becomes a prognostic factor in patients with PH (5,6). It remains uncertain if LV has metabolic remodeling as RV.

In conclusion, the current study showed that the TCA cycle was less activated because of a decreasing trend in the expression of fumaric acid, malic acid, and citric acid, which might be attributable to the expression levels of adenylosuccinic acid and argininosuccinic acid, and suggested that dysregulated BCAA metabolism and a decrease in FA oxidation might contribute to a reduction in TCA cycle reactions.

**Acknowledgements**

Not applicable.

**Funding**

The present study was supported by research grants from the Respiratory Failure Research Group (H26-Intractable diseases-General-076) from the Ministry of Health, Labour and Welfare, Japan; a grant to the Pulmonary Hypertension Research Group (grant no. 15ek0109127h0001) from the Japan Agency for Medical Research and Development (AMED); a Grant-in-Aid for Scientific Research (JSPS KAKENHI grant no. 17H04181, 19H03664).

**Availability of data and materials**

The datasets used and/or analyzed during the current study are available from the corresponding author on reasonable request.

**Authors' contributions**

SS, EK, HS, AN, HM, RS, TJS, NT and KT contributed to the study conception and design. Material preparation, data collection and analysis were performed by SS, EK, HS, AN, HM, RS, TJS, NT and KT. The first draft of the manuscript was written by SS and all authors reviewed on previous versions of the manuscript. All authors read and approved the final manuscript.

**Ethics approval and consent to participate**

All animal studies have been approved by the Review Board for Animal Experiments of Chiba University (no. 30-126) and have therefore been performed in accordance with the ethical standards laid down in the 1964 Declaration of Helsinki and its later amendments.

**Patient consent for publication**

Not applicable.

**Competing interests**

Dr Sakao has received honoraria for lectures from Nippon Shinyaku Co., Ltd.; Bayer Yakuhin, Ltd.; Actelion Pharmaceuticals, Ltd.; and Pfizer. Tanabe has received honoraria for lectures from Actelion Pharmaceuticals, Nippon Shinyaku Co., Ltd., Astellas and Pfizer and research grant support from Actelion Pharmaceuticals. Dr Tatsumi has received honoraria for lectures from Glaxo Smith Kline, Nippon Shinyaku Co., Ltd., and Actelion Pharmaceutical Ltd. and research grant support from Ono Pharmaceuticals, Ltd., Actelion Pharmaceuticals, Ltd. and Teijin Limited Teijin Ltd.

**References**

1. Davie NJ, Schermuly RT, Weissmann N, Grimminger F and Ghofrani HA: The science of endothelin-1 and endothelin receptor antagonists in the management of pulmonary arterial hypertension: Current understanding and future studies. Eur J Clin Inves 39 (Suppl): 38-49, 2009.
2. Humbert M, Morrell NW, Archer SL, Stenmark KR, MacLean MR, Lang IM, Christman BW, Weir EK, Eickelberg O, Voelkel NF and Rabinovitch M: Cellular and molecular pathobiology of pulmonary arterial hypertension. J Am Coll Cardiol 43 (12 Suppl S): 13S-24S, 2004.
3. Oka M, Homma N, Taraseviciene-Stewart L, Morris KG, Kraskauskas D, Burns N, Voelkel NF and McMurtry IF: Rho kinase-mediated vasoconstriction is important in severe occlusive pulmonary arterial hypertension in rats. Circ Res 100: 923-929, 2007.
4. Sakao S, Voelkel NF, Tanabe N and Tatsumi K: Determinants of an elevated pulmonary arterial pressure in patients with pulmonary arterial hypertension. Respir Res 16: 84, 2015.

5. van de Veerdonk MC, Kind T, Marcus JT, Mauritz GJ, Heymans MW, Bogaard HJ, Boonstra A, Marques KM, Westerhof N and Vonk-Noordegraaf A: Progressive right ventricular dysfunction in patients with pulmonary arterial hypertension responding to therapy. J Am Coll Cardiol 58: 2511-2519, 2011.
6. Freed BH, Gomberg-Maitland M, Chandra S, Mor-Avi V, Rich S, Archer SL, Jamison EB Jr, Lang RM and Patel AR: Late gadolinium enhancement cardiovascular magnetic resonance predicts clinical worsening in patients with pulmonary hypertension. J Cardiovasc Magn Reson 14: 11, 2012.
7. Paulin R and Michelakis ED: The metabolic theory of pulmonary arterial hypertension. Circ Res 115: 148-164, 2014.
8. Archer SL, Gomberg-Maitland M, Maitland ML, Rich S, Garcia JG and Weir EK: Mitochondrial metabolism, redox signaling, and fusion: A mitochondria-ROS-HIF-1alpha-Kv1.5 O2-sensing pathway at the intersection of pulmonary hypertension and cancer. Am J Physiol Heart Circ Physiol 294: H570-H578, 2008.
9. Piao L, Fang YH, Cadete VJ, Wietholt C, Urboniene D, Toth PT, Marsboom G, Zhang HJ, Haber I, Rehman J, *et al*: The inhibition of pyruvate dehydrogenase kinase improves impaired cardiac function and electrical remodeling in two models of right ventricular hypertrophy: Resuscitating the hibernating right ventricle. J Mol Med (Berl) 88: 47-60, 2010.
10. Stanley WC, Lopaschuk GD, Hall JL and McCormack JG: Regulation of myocardial carbohydrate metabolism under normal and ischaemic conditions. Potential for pharmacological interventions. Cardiovasc Res 33: 243-257, 1997.
11. Sakao S, Miyauchi H, Voelkel NF, Sugiura T, Tanabe N, Kobayashi Y and Tatsumi K: Increased right ventricular fatty acid accumulation in chronic thromboembolic pulmonary hypertension. Ann Am Thorac Soc 12: 1465-1472, 2015.
12. Sakao S, Daimon M, Voelkel NF, Miyauchi H, Jujo T, Sugiura T, Ishida K, Tanabe N, Kobayashi Y and Tatsumi K: Right ventricular sugars and fats in chronic thromboembolic pulmonary hypertension. Int J Cardiol 219: 143-149, 2016.
13. Fang YH, Piao L, Hong Z, Toth PT, Marsboom G, Bache-Wiig P, Rehman J and Archer SL: Therapeutic inhibition of fatty acid oxidation in right ventricular hypertrophy: Exploiting Randle's cycle. J Mol Med (Berl) 90: 31-43, 2012.
14. Buermans HP, Redout EM, Schiel AE, Musters RJ, Zuidwijk M, Eijk PP, van Hardeveld C, Kasanmoentalib S, Visser FC, Ylstra B and Simonides WS: Microarray analysis reveals pivotal divergent mRNA expression profiles early in the development of either compensated ventricular hypertrophy or heart failure. Physiol Genomics 21: 314-323, 2005.
15. Faber MJ, Dalinghaus M, Lankhuizen IM, Bezstarosti K, Dekkers DH, Duncker DJ, Helbing WA and Lamers JM: Proteomic changes in the pressure overloaded right ventricle after 6 weeks in young rats: Correlations with the degree of hypertrophy. Proteomics 5: 2519-2530, 2005.
16. Faber MJ, Dalinghaus M, Lankhuizen IM, Bezstarosti K, Verhoeven AJ, Duncker DJ, Helbing WA and Lamers JM: Time dependent changes in cytoplasmic proteins of the right ventricle during prolonged pressure overload. J Mol Cell Cardiol 43: 197-209, 2007.
17. Gomez-Arroyo J, Mizuno S, Szczepanek K, Van Tassell B, Natarajan R, dos Remedios CG, Drake JI, Farkas L, Kraskauskas D, Wijesinghe DS, *et al*: Metabolic gene remodeling and mitochondrial dysfunction in failing right ventricular hypertrophy secondary to pulmonary arterial hypertension. Circ Heart Fail 6: 136-144, 2013.
18. Wishart DS: Current progress in computational metabolomics. Brief Bioinform 8: 279-293, 2007.
19. Kato F, Sakao S, Takeuchi T, Suzuki T, Nishimura R, Yasuda T, Tanabe N and Tatsumi K: Endothelial cell-related autophagic pathways in Sugen/hypoxia-exposed pulmonary arterial hypertensive rats. Am J Physiol Lung Cell Mol Physiol 313: L899-L915, 2017.
20. Ohashi Y, Hirayama A, Ishikawa T, Nakamura S, Shimizu K, Ueno Y, Tomita M and Soga T: Depiction of metabolome changes in histidine-starved Escherichia coli by CE-TOFMS. Mol Biosyst 4: 135-147, 2008.
21. Ooga T, Sato H, Nagashima A, Sasaki K, Tomita M, Soga T and Ohashi Y: Metabolomic anatomy of an animal model revealing homeostatic imbalances in dyslipidaemia. Mol Biosyst 7: 1217-1223, 2011.
22. Sugimoto M, Wong DT, Hirayama A, Soga T and Tomita M: Capillary electrophoresis mass spectrometry-based saliva metabolomics identified oral, breast and pancreatic cancer-specific profiles. Metabolomics 6: 78-95, 2010.
23. Junker BH, Klukas C and Schreiber F: VANTED: A system for advanced data analysis and visualization in the context of biological networks. BMC Bioinformatics 7: 109, 2006.
24. Brunner E and Munzel U: The nonparametric Behrens-Fisher problem: Asymptotic theory and a small-sample approximation. Biom J 42: 17-25, 2000.
25. Håugaa H, Thorgersen EB, Pharo A, Boberg KM, Foss A, Line PD, Sanengen T, Almaas R, Grindheim G, Pischke SE, *et al*: Early bedside detection of ischemia and rejection in liver transplants by microdialysis. Liver Transpl 18: 839-849, 2012.
26. Ramsay RR, Gandour RD and van der Leij FR: Molecular enzymology of carnitine transfer and transport. Biochim Biophys Acta 1546: 21-43, 2001.
27. Kyoto Encyclopedia of Genes and Genomes (KEGG): Alanine, aspartate and glutamate metabolism - Mus musculus (mouse). https://www.genome.jp/kegg-bin/show_pathway?org_name=mmu&mapno=00250&mapscale=&show_description=hide. Accessed March 8, 2018.
28. Kim Y, Goto H, Kobayashi K, Sawada Y, Miyake Y, Fujiwara G, Chiba H, Okada T and Nishimura T: Detection of impaired fatty acid metabolism in right ventricular hypertrophy: Assessment by I-123 beta-methyl iodophenyl pentadecanoic acid (BMIPP) myocardial single-photon emission computed tomography. Ann Nucl Med 11: 207-212, 1997.
29. Bogaard HJ, Natarajan R, Henderson SC, Long CS, Kraskauskas D, Smithson L, Ockaili R, McCord JM and Voelkel NF: Chronic pulmonary artery pressure elevation is insufficient to explain right heart failure. Circulation 120: 1951-1960, 2009.
30. Adam J, Yang M, Bauerschmidt C, Kitagawa M, O'Flaherty L, Maheswaran P, Özkan G, Sahgal N, Baban D, Kato K, *et al*: A role for cytosolic fumarate hydratase in urea cycle metabolism and renal neoplasia. Cell Rep 3: 1440-1448, 2013.
31. Lewis GD, Ngo D, Hemnes AR, Farrell L, Domos C, Pappagianopoulos PP, Dhakal BP, Souza A, Shi X, Pugh ME, *et al*: Metabolic profiling of right ventricular-pulmonary vascular function reveals circulating biomarkers of pulmonary hypertension. J Am Coll Cardiol 67: 174-189, 2016.
32. Rhodes CJ, Ghataorhe P, Wharton J, Rue-Albrecht KC, Hadinnapola C, Watson G, Bleda M, Haimel M, Coghlan G, Corris PA, *et al*: Plasma metabolomics implicates modified Transfer RNAs and altered bioenergetics in the outcomes of pulmonary arterial hypertension. Circulation 135: 460-475, 2017.